

Published in final edited form as:

J Mol Biol. 2013 February 22; 425(4): 713–724. doi:10.1016/j.jmb.2012.12.014.

Coilin displays differential affinity for specific RNAs in vivo and is linked to telomerase RNA biogenesis

Hanna J. Broome^a and Michael D. Hebert^{*}

Department of Biochemistry, The University of Mississippi Medical Center, Jackson, MS 39216-4505, USA

Abstract

Coilin is widely known as the protein marker of the Cajal body, a subnuclear domain important to the biogenesis of small nuclear ribonucleoproteins and telomerase, complexes that are crucial to pre-messenger RNA splicing and telomere maintenance, respectively. Extensive studies have characterized the interaction between coilin and the various other protein components of CBs and related subnuclear domains, however only a few have examined interactions between coilin and nucleic acid. We have recently published that coilin is tightly associated with nucleic acid, displays RNase activity in vitro, and is re-distributed to the rRNA-rich nucleoli in cells treated with the DNA damaging agents cisplatin or etoposide. Here, we report a specific in vivo association between coilin and ribosomal RNA (rRNA), U small nuclear RNA (snRNA) and human telomerase RNA (hTR), which is altered upon treatment with DNA damaging agents. Using chromatin IP (ChIP), we provide evidence of coilin interaction with specific regions of U snRNA gene loci. We have also utilized bacterially expressed coilin fragments in order to map the region(s) important for RNA binding and RNase activity in vitro. Additionally, we provide evidence of coilin involvement in the processing of hTR both in vitro and in vivo.

Keywords

Cajal body; SMN; telomere; splicing; nucleolus

INTRODUCTION

Coilin is a protein expressed in all eukaryotic cells that is localized to the nucleus and known primarily as the Cajal body (CB) marker protein. Coilin was discovered as a result of autoantibody recognition by patient sera in 1991, and this antibody also recognized the CB (formerly the coiled body)¹. CBs, first reported in neuronal cells by Ramon y Cajal in 1903², are subnuclear domains present in cells with relatively high transcriptional demands, i.e. cancer and neurons, and contain locally high concentrations of factors required for small nuclear ribonucleoprotein (snRNP) and telomerase biogenesis^{3; 4; 5; 6; 7}. A number of the proteins that are found concentrated in the CB are also found in other distinct nuclear

© 2012 Elsevier Ltd. All rights reserved.

^{*}Address correspondence to: Michael D. Hebert, Department of Biochemistry, The University of Mississippi Medical Center, 2500 North State Street, Jackson, MS 39216-4505, Tel: (601) 984-1526, FAX: (601) 984-1501, mhebert@umc.edu.

^aDepartment of Biochemistry, The University of Mississippi Medical Center, 2500 North State Street, Jackson, MS 39216-4505, Tel: (601) 984-1856, hjohnson@umc.edu

Publisher's Disclaimer: This is a PDF file of an unedited manuscript that has been accepted for publication. As a service to our customers we are providing this early version of the manuscript. The manuscript will undergo copyediting, typesetting, and review of the resulting proof before it is published in its final citable form. Please note that during the production process errors may be discovered which could affect the content, and all legal disclaimers that apply to the journal pertain.

bodies, such as gems^{8; 9}, histone locus bodies¹⁰, and the nucleolus^{11; 12}. For example, the survival of motor neurons protein, SMN, is a component necessary for proper snRNP biogenesis that localizes to the cytoplasm in addition to the CB and/or gem in the nucleus^{13; 14}. Loss of SMN protein causes the disease spinal muscular atrophy, SMA, the leading genetic cause of infant mortality¹⁵. Another important factor found in the CB is the protein arising from the WD40 encoding RNA antisense to p53 gene, WRAP53 (also known as TCAB1 and WDR79), which functions in recruitment of telomerase to CBs and subsequently telomeres¹⁶. WRAP53 associates with coilin and plays a crucial role in CB integrity¹⁷. Additionally, the nucleolar proteins fibrillarin and Nopp140 (for “nucleolar phosphoprotein of 140 kDa), which function in the biogenesis of small nucleolar ribonucleoproteins (snRNPs), are also concentrated in the CB^{18; 19}. Interestingly, Ramon y Cajal described what we now know as CBs as “nucleolar accessory bodies” due to the fact that both the nucleolus and his accessory bodies were visible by modified silver nitrate staining², suggesting they both contain similar components. As the localization of fibrillarin and Nopp140 demonstrate, this initial observation has been proven correct.

Coilin is constitutively expressed in human cells, including those in which CBs are inconspicuous and few in number²⁰, yet despite its significance as the CB marker protein, the majority of coilin is located in the nucleoplasm outside CBs²¹. Recent studies have shed light on possible roles for nucleoplasmic coilin, such as participation in the response to DNA damage²², interaction with Ku proteins necessary for non-homologous DNA end joining²³, and relocalization in response to viral infection²⁴. However, the necessity of coilin for canonical CB formation and integrity is indisputable in that CBs cannot form without coilin in *Drosophila*²⁵, residual CBs in coilin knockout mouse cells do not contain SMN or Sm snRNPs²⁶, and coilin knockdown in HeLa cells obliterate CBs²⁷. Given the fact that the majority of coilin is non-CB localized, and that it is expressed in cells that lack CBs, it stands to reason that more exploration of coilin characteristics and activity apart from the role in CB integrity is needed. As to the necessity of coilin for overall cell or organismal viability, knockdown and knockout studies in human, mouse and zebrafish result in decreased proliferation and viability^{27; 28; 29}. In contrast, reduction of coilin in *Arabidopsis* and *Drosophila* does not result in any obvious phenotype apart from no CBs^{25; 30}.

Coilin has been shown to interact with SMN, which facilitates the biogenesis of snRNPs by aiding in the addition of a septet of Sm proteins onto snRNA in the cytoplasm of cells^{31; 32; 33}. snRNPs form the core of the spliceosome, which functions in the removal of intronic sequences from hnRNA and the splicing together of exons in order to form mRNA. snRNA, the RNA component of the snRNP, undergoes base modifications guided by small Cajal body specific RNA (scaRNA) in the CB during the final steps of the snRNP maturation process, in addition to 3' processing by the Integrator complex which occurs co-transcriptionally^{34; 35; 36; 37}. It has been shown that CBs co-localize with certain gene loci, including those for U1 and U2 snRNA^{38; 39}, and this co-localization is mediated by active transcription of U snRNA^{40; 41}. Interestingly, not only are snRNAs targeted to the CB immediately upon re-entry from the cytoplasm³⁴, but nascent U snRNA transcripts transit through the CB prior to assembly with the nuclear export complex⁴². In addition to snRNAs, the RNA subunit of human telomerase (hTR) has been found in relatively high concentrations within the CBs of cancerous cells and is known to undergo similar 3' processing to that of U1 and U2 snRNAs^{3; 43}. It has been shown that coilin knockdown disrupts recruitment of endogenous telomerase to telomeres, and mutation of the CB localization signal in hTR abrogates both telomerase recruitment and telomere extension^{16; 44}. In *S. cerevisiae*, the spliceosome is responsible for the processing of telomerase RNA⁴⁵, however the mechanism for hTR processing remains elusive. As stated above, a number of excellent studies have been done on the interaction between coilin and the numerous other protein components of the CB, while few have explored the relationship

between coilin and nucleic acids^{24; 46; 47}. Considering that coilin binds both DNA and RNA and has RNase activity (Broome and Hebert, 2012), we explore here the association of coilin with various RNAs and gene loci. Our previous results suggest that there is likely much to discover in terms of the relationship not only between coilin and DNA/RNA in the context of the CB, but also within the nucleoplasm as a whole.

RESULTS

Coilin associates with specific RNA and DNA in the cell

Despite the lack of a canonical RNA binding domain, several studies provide evidence of a link between RNA and coilin. *Xenopus* coilin has been shown to associate with specific RNA homopolymers⁴⁶, human coilin is localized to the rRNA-rich nucleolus in cells treated with DNA damaging agents^{22; 48}, and bacterially expressed coilin remains bound to RNA throughout a very stringent purification protocol⁴⁷. Therefore, we wanted to explore the association of coilin with specific RNA transcripts, in both untreated and stressed cells, by immunoprecipitation (IP) of coilin followed by RNA isolation from the IP complex and analysis by quantitative real-time reverse transcriptase PCR (qRT-PCR). We examined the association between the coilin IP complex and six different RNAs in HeLa cells. GAPDH RNA was used as a negative control since it is not enriched in the CB. Pre-processed 47/45S and processed 5.8S ribosomal RNAs (rRNA) were examined due to the relationship between coilin and the nucleolus, especially in stress conditions. U1 and U2 snRNA and the RNA subunit of telomerase (hTR) were analyzed due to their enrichment in the CB. In untreated cells, a significant association was seen between coilin and 47/45S pre-rRNA, U2 snRNA and hTR (Figure 1A) compared to the amount of these transcripts recovered from the control IgG IP. There was variation in the amount of recovery between these three messages, with a 2 fold enrichment of 47/45S pre-rRNA in the coilin IP over the control IgG IP, a 3.6 fold enrichment of U2 snRNA and a striking 17.5 fold enrichment of telomerase RNA.

In addition, we also wanted to examine any changes in coilin association with RNA that occur in cells treated with DNA damaging agents. For these experiments we utilized etoposide and cisplatin, which we have previously shown result in the nucleolar accumulation of coilin^{22; 48}. Based on this observed alteration in coilin localization, we hypothesized that treatment with etoposide or cisplatin would result in an increased association between coilin and rRNA and a decreased association between coilin and the CB enriched snRNA and hTR transcripts. Indeed we found that in both etoposide and cisplatin treated cells an increased association was observed between coilin and rRNA, without a significant change in the relative recovery of GAPDH RNA (Figure 1A). In etoposide treated cells, the fold enrichment increased from 2 to 4.9 for 47/45S pre-rRNA and from 1.2 to 3.4 for 5.8S rRNA. Cisplatin treatment resulted in a dramatic increase from 2 to 10.6 fold enrichment of 47/45S pre-rRNA without a significant change in the recovery of 5.8S rRNA. However, in contrast to our hypothesis, etoposide and cisplatin treatments resulted in increased association between coilin and U1 and U2 snRNA. Most notably, etoposide treatment resulted in a substantial increase of coilin complex association with U2 snRNA, from 3.6 fold over IgG in untreated cells to 13.6 fold in etoposide treated cells. Moreover, hTR association with the coilin complex was likewise increased upon cisplatin treatment compared to that seen in untreated cells (to 28 fold over that recovered by control IgG). In contrast, the recovery hTR from the coilin IP complex was not significantly different in etoposide treated versus untreated cells.

To examine the efficacy of our IP protocol, we used antibodies to the nucleolar/CB protein fibrillarin as well as the cytoplasmic/CB protein SMN and examined the association of these protein complexes with the same six RNA transcripts tested above. Given the roles for fibrillarin and SMN in snoRNP and snRNP biogenesis, respectively, we hypothesized that

fibrillarin would associate most with rRNA while SMN would IP predominantly U1 and U2 snRNAs. As expected, IP with α -fibrillarin resulted in an 18.3 fold enrichment of 47/45S rRNA and a 3.6 fold enrichment 5.8S rRNA relative to IgG control (Figure 1B). The fibrillarin complex was also found to significantly associate with U2 snRNA (4.2 fold enrichment) and hTR (7.8 fold enrichment) relative to IgG control. The fact that fibrillarin localizes to both CBs and the nucleolus likely accounts for these associations. SMN IP enriched for U1 snRNA at 2.9 fold over IgG, without a significant enrichment for U2 or any other RNA. It has been published that U1 snRNA are two times more abundant than U2 snRNA⁴⁹, which most likely accounts for why we do not see a significant enrichment for U2 by SMN. It is worth noting that there was significantly more GAPDH RNA associated with fibrillarin than with SMN, suggesting that IPs for fibrillarin inherently enrich for RNA, emphasizing the specific U1 snRNA enrichment by SMN. Interestingly, although both fibrillarin and SMN, like coilin, are found in other cellular locations in addition to their accumulations in CBs, neither of these protein complexes was enriched as much for hTR compared to that found for coilin IP (17.5 fold).

Given that coilin is known primarily for its role in CB formation and composition, we wanted to explore whether coilin would also associate with specific RNA transcripts in cell lines lacking CBs. For these studies, we used the primary human lung fibroblast cell line WI-38. CBs are observed in less than 3% of WI-38 cells⁵⁰ and these CBs are smaller and fewer in number to those found in transformed cell lines, such as HeLa. We performed coilin and control IPs using WI-38 cells as shown in Figure 1C. In this cell line, coilin significantly enriches for both rRNA transcripts as well as U2 snRNA, suggesting that nucleoplasmic coilin can participate in these RNA associations. As expected, hTR levels were undetectable in isolated RNA from WI-38 cells (our unpublished results), therefore we did not examine the presence of this transcript in coilin IP samples from this cell line.

It has been shown in HeLa cells that CBs associate non-randomly with U1 and U2 gene loci as well as certain histone gene loci^{38; 39}. We hypothesized that due to the DNA binding ability of coilin⁴⁷, it may serve as a link between the CB and these gene loci. Using the ChIP assay with endpoint analysis using quantitative real-time PCR (qPCR) and specific primers, we have determined that coilin interacts most with the 3' end of U2 (Figure 2). This data demonstrates not only an *in vivo* association between coilin and specific DNA, but also supports our previously published suggested role of coilin in the processing of snRNA at transcription sites⁴⁷.

Differential solubility and nucleic acid binding of wild type coilin and mutants

Previously, we have observed that bacterially expressed coilin co-purifies with nucleic acid⁴⁷ and when incubated with DNase and RNase, precipitates out of solution (Supplemental Figure 1). In order to map the region(s) of coilin responsible for nucleic acid binding, we next tested various fragment and deletion constructs that were partially purified from *E. coli*. We have found clear differences for seven bacterially expressed coilin proteins partially purified by GST-tag in regards to bound nucleic acid and precipitation following nuclease treatment (Figure 3A). When full-length coilin, the N-terminal fragment N362 or the deletion construct Δ 241-291 are treated with nucleases, a white precipitate is observed (Figure 3, A and D). Much less precipitate is observed in constructs that lack either residues 121-291 or the 94 amino terminal residues that contain the self-association domain. This suggests that both the self-association domain and residues 121-241 contribute to the precipitation driven by nucleic acid removal. Preliminary experiments provided clear evidence that the white precipitate observed was in fact protein, however, we wanted to examine the total loss of each tested protein during precipitation following DNase and RNase treatment. Due to the presence of truncation products present in the partially purified proteins, equal amounts of total protein was subjected to SDS-PAGE followed by

Coomassie staining (Figure 3B, top panel). With the exception of the Δ 241-291 protein, near equal amounts of full-length proteins (marked by *) are present in each lane. Following nuclease treatment, precipitated protein was pelleted by centrifugation and equal volumes of remaining soluble fraction was loaded to demonstrate the relative protein loss in precipitation for each construct (Figure 3B, bottom panel). As expected, the most drastic loss of full-length protein was seen in proteins that demonstrate the most visible precipitate increase with nuclease treatment, namely full-length coilin, N362 and Δ 241-291. Additionally, we analyzed equal amounts of partially purified proteins for relative amounts of co-purified nucleic acid as visible by ethidium bromide staining (Figure 3C). We have previously shown that the majority of nucleic acid co-purified with coilin is RNA⁴⁷. Density analysis indicates that constructs lacking any part of the 121-291 region co-purify with the least amount of RNA, suggesting that the 121-291 region may be primarily responsible for RNA binding. Additionally, constructs lacking the self-association domain in the first 94 residues (94-576 and 94-291) co-purify with the most nucleic acid, suggesting a suppressing effect of this domain on RNA binding. Figure 3D demonstrates the necessity of RNA over DNA for maintaining protein solubility of full length coilin, which agrees with our previous observations⁴⁷ that the majority of the co-purified nucleic acid is RNA.

RNase activity of nucleic acid free wild type coilin and mutants

We have previously published a coilin purification protocol of bacterially expressed GST fusion proteins that yields a pure protein of single band homogeneity by SDS-PAGE, and that coilin purified by this method displays RNase activity *in vitro*⁴⁷. Additionally, we found that purified coilin remains bound to both DNA and RNA, despite the stringency of the protocol. In order to examine the RNase activity of coilin protein alone, in the absence of nucleic acid, we modified our purification protocol to include treatment with DNase and RNase. As stated above, treatment with nucleases results in visible protein precipitation. We found that DNase/RNase treatment of the partially purified protein prior to electroelution results in diminished RNase activity of purified coilin (our unpublished results). We suspected that more SDS binds coilin when nucleic acid has been removed, therefore we stripped the excess SDS by incubation with α -cyclodextrin and indeed the RNase activity was increased, albeit not to the level seen with nucleic acid-bound coilin. Following incubation with α -cyclodextrin, the soluble protein is dialyzed in order to remove the α -cyclodextrin/SDS complexes and to buffer change into 1X PBS containing 250 mM NaCl, a necessary salt amount for protein solubility. Supplemental Figure 2 contains nucleic acid free wild type coilin at various steps during the modified protocol subjected to SDS-PAGE and Coomassie staining. This modified protocol yields nucleic acid free purified coilin, visible as a single band by Coomassie staining following SDS-PAGE, which displays RNase activity.

Coilin contains none of the canonical domains present in other proteins with RNase and DNA binding activities, however, we have recently published that coilin displays both these activities *in vitro*⁴⁷. The RNase activity seems to be localized to the N-terminus of coilin, as C-terminal fragments do not produce comparable RNA degradation to either full-length or an N-terminal fragment. To further examine the region(s) of coilin necessary for RNase activity, and fit this to the nucleic acid binding and solubility data from Figure 3, we purified various coilin proteins using the previously described protocol to obtain GST-tagged nucleic acid free proteins (Figure 4A, listed in Figure 3A). Equivalent amounts of these proteins were incubated with a fixed amount of HeLa RNA, subjected to electrophoresis through agarose and stained with ethidium bromide (Figure 4B). Drastic degradation is observed with increasing amounts of full-length coilin as well as with the 94-576 and N362 fragments (top panels). Visibly less degradation is seen in the incubations with the 94-291 fragment and deletion mutant Δ 121-291 and little to no visible degradation is observed with the C214

fragment (bottom panels). Densitometry of the 28S rRNA band from each incubation shown in Figure 4B was plotted to show the relative degradation with increasing amounts of each protein (Figure 4C). As expected, the most drastic decrease in band intensity is in the full-length, N362 and 94-576 incubations, followed closely by the 94-291 incubation. The least active N-terminal-containing mutant is Δ 121-291, and only a slight decrease in band intensity is seen with the C214 incubations. Interestingly, the partially purified Δ 121-291 mutant also bound the least relative amount of RNA and remained soluble following nuclease treatment (Figure 3), suggesting functional and structural importance inherent to this region of coilin.

In vitro processing of telomerase RNA by coilin

Since our previous studies on in vitro processing of specific RNA transcripts had been with purified coilin containing nucleic acid⁴⁷, we wanted to examine the activity of nucleic acid free full length coilin. Incubations were performed with increasing protein and a fixed amount of HeLa total RNA (Figure 5A), showing that cleavage of the GST tag followed by DNase and RNase treatment and completion of the purification protocol results in more RNase activity (Figure 5A, 0.15 μ g protein) relative to identically purified protein with GST tag intact (Figure 4C, top left panel, 0.7 μ g protein). To continue exploring the functionality of coilin RNase activity, we hypothesized that perhaps the reason coilin binds such a drastic amount of telomerase RNA is due to its participation some aspect of its biogenesis. It has been shown that the RNA component of the telomerase enzyme, hTR, localizes to the CB in human cancer cells and undergoes a processing event at the 3' end by an unknown mechanism^{3:43}. The similarities between snRNA and telomerase RNA, including localization to the CB, led us to hypothesize that coilin might play a role in the processing of hTR. We therefore incubated nucleic acid free purified coilin (cleaved from GST) with HeLa total RNA, and examined the amount of total hTR and pre-processed hTR (pre-hTR) using specific primers by qRT-PCR (Supplemental Figure 3). Figure 5B shows that relative to the control incubation, HeLa RNA incubated with coilin contains 64% less pre-hTR with only a slight insignificant decrease in total hTR. We also hypothesized that the coilin mutants Δ 121-291 and C214, which showed little total RNase activity and decreased RNA binding (Figures 3 and 4), would also be deficient in processing the pre-hTR in vitro when compared to full-length coilin. In order to make direct comparisons between full length coilin and these mutants, we utilized the same GST-tagged constructs shown in Figure 4B. As expected, comparison of the GST-tagged nucleic acid free purified proteins show that full-length coilin reduces pre-hTR by 50%, but no significant reduction of pre-hTR was observed in either the Δ 121-291 or C214 reactions (Figure 5C). These experiments show the preference of coilin for degradation of pre-processed hTR, as well as the necessity of the N-terminal amino acids 121-291 for this in vitro activity.

Pre-processed telomerase RNA abundance linked to coilin levels

Due to the evidence of in vitro pre-hTR processing by coilin, we hypothesized that coilin overexpression and knockdown would result in a decrease and increase, respectively, of pre-hTR levels in the cell. We therefore transfected HeLa cells for 24 h with either GFP-coilin wild type or empty GFP vector, harvested the cells, isolated the RNA and analyzed hTR and pre-hTR levels using specific primers by qRT-PCR. In addition, we treated HeLa cells for 48 h with either an siRNA targeting coilin mRNA or a non-targeting control siRNA and analyzed the RNA in the same manner as described above. As expected, overexpression of GFP-coilin resulted in a 68% reduction in pre-hTR, however the total hTR was also decreased by 42% (Figure 6A). Somewhat unexpectedly, we observed a 46% decrease in pre-hTR levels following a 48 h coilin knockdown that resulted in an 89% reduction in coilin mRNA (Figure 6B). Collectively, these results are intriguing, as they point to the involvement of coilin, whether direct or indirect, in the processing of hTR.

DISCUSSION

Since the discovery of coilin in 1991, numerous studies have revealed interactions between the CB marker protein and proteins important for many processes, such as snRNA biogenesis^{33; 51}, rRNA biogenesis^{12; 22}, and non-homologous DNA end joining²³. In contrast, far fewer papers have been published on the association between coilin and specific RNAs. Here we report a striking association between coilin and telomerase RNA (Figure 1), a transcript that is known to be concentrated in the CB for interaction with WRAP53 and assembly of the telomerase holoenzyme^{3; 7; 17}. Additionally, we show that coilin binds pre-rRNA and U2 snRNA (Figure 1). Treatment with DNA damaging agents cisplatin and etoposide have been shown to redistribute coilin to the nucleolus of primary and transformed cell lines^{22; 48}, and we have shown that this correlates with an increase in rRNA transcripts co-immunoprecipitated with coilin (Figure 1). We previously published evidence of coilin's response to DNA damaging agents that involves an interaction with RNA polymerase I and suppression of its activity²². The RNA IP experiments reported here reveal the potential for an additional mechanism of coilin-mediated response to cell stress that is centered upon rRNA processing or stability.

We have recently published the DNA-binding activity of bacterially expressed coilin⁴⁷, and it has been shown that a significant association occurs between CBs and U1 and U2 gene loci^{38; 39}. The ChIP data provided in this study (Figure 2) suggest an additional mechanism for CB co-localization with gene loci, mediated by the coilin-DNA interaction, and also support our previous proposed model of coilin involvement in co-transcriptional U snRNA processing. Previous studies have shown that α -coilin ChIP enriches for regions of damaged centromeric DNA in virus infected cells²⁴. Also, alteration of coilin levels affect RNA polymerase I occupancy of ribosomal DNA, which may play a role in the mechanism for suppression of rRNA transcription following DNA damage²². These studies suggest that cell stress can influence both the association between coilin and DNA, as well as coilin-mediated association between DNA and other proteins.

Although it has been shown that coilin binds DNA and RNA^{24; 46; 47}, it lacks any canonical domains present in other nucleic acid binding proteins. By sequence analysis, coilin is predicted to be intrinsically disordered throughout the intermediate region of the protein, with order in the more highly conserved N- and C-termini⁴⁷. Using bacterially expressed coilin fragments, we show that amino acids 121-291 in the intermediate disordered region of the protein are functional in protein solubility, RNA binding, and RNase activity. Additional structural and mutational studies are needed to determine the alteration of protein conformation that occurs upon RNA binding, and determine specific residues required for RNase activity.

We also show that while fibrillarin and SMN enrich for hTR in HeLa cells, the association of this transcript with coilin is markedly more significant. Why does coilin enrich for hTR much more than fibrillarin and SMN when all three of these proteins are found in the CB? Previous studies report the interaction between coilin and the protein WRAP53, which is responsible for hTR and scaRNA localization to the CB^{16; 17}. The association reported here between coilin and hTR suggest the possibility that hTR mediates the interaction between coilin and WRAP53. Alternatively, coilin may interact directly with WRAP53, which can also associate with hTR.

There is an extensively published relationship between telomerase biogenesis and the CB, including failure of telomerase recruitment to telomeres and telomere extension resulting from failure of hTR to transit through the CB or disruption of the CB^{3; 7; 16; 43; 44}. WRAP53, the protein required for telomerase recruitment to telomeres, is concentrated in

the CB, but here we provide evidence of an additional link between hTR and the CB – an interaction between coilin and the RNA. Although *S. cerevisiae* telomerase RNA is processed by the spliceosome, the mechanism by which mature hTR is generated through 3' processing of a longer transcript has yet to be elucidated⁴⁵. In this study we provide evidence of coilin participation in this event, both by in vitro reactions and by alteration of coilin levels in the cell. We link the importance of the intermediate residues 121-291 of coilin in RNA binding and total RNase activity to the processing of hTR in vitro, in that deletion of this region results in dramatic abrogation of activity. Future work is necessary to fully understand the mechanism coilin plays in the biogenesis of telomerase RNA, and whether this role is direct or indirect. The data presented here support a direct role. In addition, it will also be of interest to determine how the interaction between coilin and various specific RNA transcripts is regulated.

MATERIALS AND METHODS

Cell culture, DNA constructs and transfections

Human cervical carcinoma (HeLa) and normal human fetal lung fibroblast (WI38) cells were obtained from the American Type Culture Collection (Manassas, VA, USA). Cell lines were cultured as described⁵². Cells were transfected with GFP expression vectors⁵³ using Fugene HD Transfection Reagent (Promega, Madison, WI, USA) following the manufacturer's suggestion protocol. GST-proteins (FL coilin, N362, C214) were cloned into pGEX vectors as previously described⁴⁷. GST-Δ241-291 protein was generated by overlapping primer mutagenesis using Hercules II DNA polymerase (Agilent, Santa Clara, CA, USA) with pGEX-2T-coilin as template using the following primers: 5' - ATCGTCGCAGGATCCGACAACTGGCTATAAACTTGGC-3' and 5' - GGATCCTGCGACGATTGAGCAAACGCTTACACTACCTTTC-3'. GST-Δ121-291 was generated by overlapping primer mutagenesis as described above using pGEX-2T-coilin as template with the following primers: 5' - ATCGTCGCAGGATCCGACAACTGGCTATAAACTTGGC-3' and 5' - GGATCCTGCGACGATTTCCACCCTCCTCTAACTGAAATGC-3'. Both GST-94-576 and GST-94-291 constructs were cloned into pGEX-2T vector from their respective eGFP-C1 constructs by digestion with *Bam*HI and *Bgl*III restriction enzymes and ligation with T4 DNA Ligase, both from New England BioLabs (Ipswich, MA, USA), using standard cloning techniques. GFP-94-576 was generated by restriction digest of pGEX-6p1-coilin and eGFP-C1-NLS (nuclear localization signal) with *Eco*RI and *Bam*HI followed by ligation as described above. GFP-94-291 was generated by restriction digest of eGFP-C1-coilin and eGFP-C1-NLS with *Eco*RI and *Pst*I followed by ligation as described above.

RNAi and drug treatment

Coilin siRNA⁵⁴ was obtained from Integrated DNA Technology (Coralville, IA, USA). The non-targeting, control siRNA⁵⁵ was obtained from Thermo Scientific (LaFayette, CO, USA). The siRNA transfections were carried out using Lipofectamine 2000 (Invitrogen, Carlsbad, CA, USA) according to the manufacturer's protocol. Drug treatments were cisplatin (3 μg/ml) for 16 hours or etoposide (20 μM) for 16 hours.

RNA-IPs

In RNA IP experiments for endpoint qRT-PCR analysis, approximately 20 million cells were lysed in 1 mL RIPA buffer (50 mM Tris-HCl pH 7.6, 150 mM NaCl, 1% NP-40, 0.25% sodium deoxycholate, 0.1% SDS, 1 mM EDTA) containing protease inhibitor cocktail (Roche, Indianapolis, IN, USA). Sonication was performed four times for 5 sec each at 4 W using the Fisher Scientific Sonic Dismembrator Model 100, followed by centrifugation for 5 min at 16000 g at 4°C. Approximately 20 million cells worth of sonicate

was used for each IP reaction, to which the respective antibody and 45 μL 50% Protein G Sepharose beads (GE Healthcare, Pittsburgh, PA, USA) were added and incubated at 4°C for approximately 18 hr on a multi-tube rotator. Normal rabbit IgG (sc-2027), α -coilin H300 rabbit polyclonal (sc-32860) and α -SMN H195 rabbit polyclonal (sc-15320) antibodies were purchased from Santa Cruz Biotechnology (Santa Cruz, CA, USA); 5 μg of each antibody was used per IP. α -Fibrillarin rabbit polyclonal antibody AB5821 was purchased from Abcam (Cambridge, MA, USA) and 4 μg was used per IP. Following the IP incubation, antibody/bead complexes were pelleted at 16000 g for 1 min, supernatant aspirated and resuspended in 1 mL RIPA buffer. This process was repeated for a total of 3 washes, after the third wash was aspirated, RNA was isolated from the antibody/bead complex using a modified Ambion RNAqueous kit protocol (Life Technologies, Carlsbad, CA, USA). Briefly, 350 μL lysis buffer was added to the beads followed by 350 μL 64% ethanol and the subsequent steps performed per the suggested protocol. RNA was eluted in a total of 100 μL elution buffer. Following elution, samples were incubated at 37°C for 30 min with TURBO DNase (Life Technologies, Carlsbad, CA, USA). Equal volumes of isolated RNA were used for the qRT-PCR analysis.

Chromatin immunoprecipitation (ChIP)

The EZ ChIP kit from Millipore (Billerica, MA, USA) was used for all ChIP experiments and the manufacturer's suggested protocol was followed. Approximately 9 million HeLa cells were used for the protocol, and lysate sonicated using a Fisher Scientific Sonic Dismembrator Model 100 four times for 10 sec on setting four. Normal rabbit IgG and α -RNA polymerase II were supplied with EZ ChIP kit; 5 μg and 1 μg were used per IP, respectively. α -coilin H300 antibody was purchased from Santa Cruz Biotechnologies; 5 μg was used per IP. Following the suggested DNA elution in 50 μL , equal volumes were used in qPCR reactions.

Bacterially expressed proteins

Partially purified GST-tagged coilin proteins were obtained by transformation into *Escherichia coli* BL21(DE3)pLysS cells, induction and purification over glutathione sepharose beads (GE Healthcare, Pittsburgh, PA, USA) as per the manufacturer's protocol. Concentration of partially purified GST-tagged proteins was estimated using BioRad Protein Assay (Hercules, CA, USA). Equal concentrations of protein were incubated with or without DNase I and RNase A/T1 cocktail (Invitrogen, Carlsbad, CA, USA) at 37°C for 30 min then centrifuged at 16000 g for 5 min to visualize protein precipitation. Equal concentrations of untreated proteins were subjected to SDS-PAGE followed by Coomassie staining; proteins were then nuclease treated and centrifuged as described above and equal volumes of the soluble protein subjected to SDS-PAGE and Coomassie staining. Equal protein concentrations were loaded into a 1% agarose gel containing ethidium bromide to visualize co-purified nucleic acid. GST-tagged coilin proteins were purified to SDS-PAGE single band homogeneity as previously described⁴⁷, with minor changes: prior to separation by SDS-PAGE, protein was incubated at 37°C for 30 min with DNase I and RNase A/T1 cocktail. After SDS-PAGE, band excision, and electro-elution, the protein was concentrated using a centrifugal filter unit (50K molecular weight cutoff (MWCO), Millipore, Billerica, MA, USA). The concentrated, electro-eluted, nucleic acid free coilin protein was incubated on ice for 30 min at a final concentration of 21 mM α -cyclodextrin⁵⁶ and 250mM NaCl to remove residual SDS. Following incubation, the reaction was centrifuged for 5 min at 16000 g, and the supernatant dialyzed against 1X PBS high salt buffer containing 10 mM Na_2HPO_4 , 1.8 mM NaH_2PO_4 and 250 mM NaCl. Dialysis was performed using a 10K MWCO Pierce Slide-A-Lyzer Dialysis Cassette from Thermo Scientific (Waltham, MA, USA) following the manufacturer's suggested protocol. Concentration of dialyzed proteins

was estimated using Pierce BCA Protein Assay Kit (Thermo Scientific, Waltham, MA, USA) following the manufacturer's protocol.

RNase assays – agarose endpoint and re-isolation endpoint for qRT-PCR

RNase assays for agarose gel endpoint analysis were conducted with 500 ng HeLa RNA isolated using the Macherey-Nagel NucleoSpin RNA II kit (Clontech, Mountain View, CA, USA) and up to 720 ng bacterially expressed protein purified as described above. Incubations were at 37°C for 30 min, loaded into a 1% agarose gel and visualized by ethidium bromide. Densitometry of gel bands was measured using Quantity One software. RNase assays for re-isolation of RNA and qRT-PCR endpoint analysis were conducted with 1.5–2.5 µg RNA and 500–800 ng protein (3:1 ratio of RNA to protein) at 37°C for 30 min. RNA was re-isolated from protein incubations using a modified protocol for the Nucleospin RNA II or AmbionRNAqueous kit (Life Technologies, Carlsbad, CA, USA); briefly, 1.5x reaction volume of lysis buffer was added followed by addition of ethanol to final 32–35%. Elution of the RNA was done in 40–60 µL. The concentration of re-isolated RNA was estimated using the Nanodrop 2000 and normalized prior to qRT-PCR analysis.

qRT-PCR (RNA IP, RNase assays, knockdowns, GFP transfections) and qPCR (ChIP)

Brilliant II SYBR Green qRT-PCR Master Mix Kit from Agilent (Santa Clara, CA, USA) was used for analysis of RNA from RNA IP experiments, RNase assays, and transfected cells. Brilliant II SYBR Green qPCR Master Mix was used for analysis of ChIP DNA. Reaction conditions and thermal cycling was done according to the manufacturer's suggested protocol. Primers for GAPDH, 47/45S pre-ribosomal RNA, U1 and U2 snRNA have been previously described^{22; 47; 57}. Primer sequences for 5.8S ribosomal RNA are 5'-CGGCTCGTGCATCGAT-3' forward and 5'-CCGCAAGTGC GTTCGAA-3' reverse; for telomerase RNA (hTR), 5'-AAATGTCAGCTGCTGGCCCGTTCG-3' forward and 5'-ACCCGCGGCTGACAGAGCCCAAC-3' reverse; and for pre-processed telomerase RNA (pre-hTR), 5'-AGGTTTCAGGCCTTTCAGGCCGAG-3' forward and 5'-GACGGATGCGCACGATCGGCGTTC-3' reverse. Primer concentrations were 140 nM for all qRT-PCR and qPCR reactions. The Stratagene Mx3000P Real Time PCR System was used with Agilent MxPro software for real-time analysis using Windows Excel for post hoc statistical analysis. The Student's T-test was used for calculation of p values.

Supplementary Material

Refer to Web version on PubMed Central for supplementary material.

Acknowledgments

We thank Dr. Andrew S. Gilder for engineering the GST-94-576, GST-94-291, GST-Δ121-291 and GST-Δ241-291 coilin constructs. We also thank Dr. Venkatramreddy Velma and Zunamys I. Carrero for their constructive comments on the manuscript. This work was supported by a grant (R01GM081448) from the National Institute of General Medical Sciences, National Institutes of Health.

ABBREVIATIONS

CB	Cajal body
ChIP	chromatin immunoprecipitation
hTR	human telomerase RNA
snRNP	small nuclear ribonucleoprotein

snRNA	small nuclear ribonucleic acid
SMN	Survival of motor neuron protein
qRT-PCR	quantitative real-time reverse transcriptase PCR
rRNA	ribosomal RNA
WRAP53	WD40 encoding RNA antisense to p53 gene

References

1. Andrade LEC, Chan EKL, Raska I, Peebles CL, Roos G, Tan EM. Human autoantibody to a novel protein of the nuclear coiled body: Immunological characterization and cDNA cloning of p80 coilin. *J Exp Med.* 1991; 173:1407–1419. [PubMed: 2033369]
2. Ramón y Cajal SR. Un sencillo metodo de coloracion selectiva del reticulo protoplasmico y sus efectos en los diversos organos nerviosos de vertebrados y invertebrados. *Trab Lab Invest Biol (Madrid).* 1903; 2:129–221.
3. Zhu Y, Tomlinson RL, Lukowiak AA, Terns RM, Terns MP. Telomerase RNA accumulates in Cajal bodies in human cancer cells. *Mol Biol Cell.* 2004; 15:81–90. [PubMed: 14528011]
4. Morris GE. The Cajal body. *Biochim Biophys Acta.* 2008; 1783:2108–15. [PubMed: 18755223]
5. Matera AG, Izaguirre-Sierra M, Praveen K, Rajendra TK. Nuclear bodies: random aggregates of sticky proteins or crucibles of macromolecular assembly? *Dev Cell.* 2009; 17:639–47. [PubMed: 19922869]
6. Tycowski KT, Shu MD, Kukoyi A, Steitz JA. A conserved WD40 protein binds the Cajal body localization signal of scaRNP particles. *Mol Cell.* 2009; 34:47–57. [PubMed: 19285445]
7. Venteicher AS, Abreu EB, Meng Z, McCann KE, Terns RM, Veenstra TD, Terns MP, Artandi SE. A human telomerase holoenzyme protein required for Cajal body localization and telomere synthesis. *Science.* 2009; 323:644–8. [PubMed: 19179534]
8. Matera AG. RNA splicing: More clues from Spinal Muscular Atrophy. *Curr Biol.* 1999; 9:R140–R142. [PubMed: 10074419]
9. Gall JG. The centennial of the Cajal body. *Nat Rev Mol Cell Biol.* 2003; 4:975–80. [PubMed: 14685175]
10. Nizami Z, Deryusheva S, Gall JG. The Cajal body and histone locus body. *Cold Spring Harb Perspect Biol.* 2010; 2:a000653. [PubMed: 20504965]
11. Raska I, Ochs RL, Andrade LEC, Chan EKL, Burlingame R, Peebles C, Gruol D, Tan EM. Association between the nucleolus and the coiled body. *J Struct Biol.* 1990; 104:120–127. [PubMed: 2088441]
12. Isaac C, Yang Y, Meier UT. Nopp140 functions as a molecular link between the nucleolus and the coiled bodies. *J Cell Biol.* 1998; 142:407–417.
13. Meister G, Buhler D, Pillai R, Lottspeich F, Fischer U. A multiprotein complex mediates the ATP-dependent assembly of spliceosomal U snRNPs. *Nat Cell Biol.* 2001; 3:945–9. [PubMed: 11715014]
14. Pellizzoni L, Yong J, Dreyfuss G. Essential Role for the SMN Complex in the Specificity of snRNP Assembly. *Science.* 2002; 298:1775–9. [PubMed: 12459587]
15. Faustino NA, Cooper TA. Pre-mRNA splicing and human disease. *Genes Dev.* 2003; 17:419–37. [PubMed: 12600935]
16. Stern JL, Zyner KG, Pickett HA, Cohen SB, Bryan TM. Telomerase recruitment requires both TCAB1 and Cajal bodies independently. *Mol Cell Biol.* 2012; 32:2384–95. [PubMed: 22547674]
17. Mahmoudi S, Henriksson S, Weibrecht I, Smith S, Soderberg O, Stromblad S, Wiman KG, Farnebo M. WRAP53 is essential for Cajal body formation and for targeting the survival of motor neuron complex to Cajal bodies. *PLoS Biol.* 2010; 8:e1000521. [PubMed: 21072240]

18. Raska I, Andrade LEC, Ochs RL, Chan EKL, Chang C-M, Roos G, Tan EM. Immunological and ultrastructural studies of the nuclear coiled body with autoimmune antibodies. *Exp Cell Res.* 1991; 195:27–37. [PubMed: 2055273]
19. Meier UT, Blobel G. NAP57, a mammalian nucleolar protein with a putative homolog in yeast and bacteria. *J Cell Biol.* 1994; 127:1505–1514. [PubMed: 7798307]
20. Young PJ, Le TT, thi Man N, Burghes AH, Morris GE. The relationship between SMN, the spinal muscular atrophy protein, and nuclear coiled bodies in differentiated tissues and cultured cells. *Exp Cell Res.* 2000; 256:365–74. [PubMed: 10772809]
21. Lam YW, Lyon CE, Lamond AI. Large-scale isolation of Cajal bodies from HeLa cells. *Mol Biol Cell.* 2002; 13:2461–73. [PubMed: 12134083]
22. Gilder AS, Do PM, Carrero ZI, Cosman AM, Broome HJ, Velma V, Martinez LA, Hebert MD. Coilin participates in the suppression of RNA polymerase I in response to cisplatin-induced DNA damage. *Mol Biol Cell.* 2011; 22:1070–9. [PubMed: 21289084]
23. Velma V, Carrero ZI, Cosman AM, Hebert MD. Coilin interacts with Ku proteins and inhibits in vitro non-homologous DNA end joining. *FEBS Lett.* 2010; 584:4735–9. [PubMed: 21070772]
24. Morency E, Sabra M, Catez F, Texier P, Lomonte P. A novel cell response triggered by interphase centromere structural instability. *J Cell Biol.* 2007; 177:757–68. [PubMed: 17548509]
25. Liu JL, Wu Z, Nizami Z, Deryusheva S, Rajendra TK, Beumer KJ, Gao H, Matera AG, Carroll D, Gall JG. Coilin is essential for Cajal body organization in *Drosophila melanogaster*. *Mol Biol Cell.* 2009; 20:1661–70. [PubMed: 19158395]
26. Tucker KE, Berciano MT, Jacobs EY, LePage DF, Shpargel KB, Rossire JJ, Chan EK, Lafarga M, Conlon RA, Matera AG. Residual Cajal bodies in coilin knockout mice fail to recruit Sm snRNPs and SMN, the spinal muscular atrophy gene product. *J Cell Biol.* 2001; 154:293–307. [PubMed: 11470819]
27. Lemm I, Girard C, Kuhn AN, Watkins NJ, Schneider M, Bordonne R, Luhrmann R. Ongoing U snRNP biogenesis is required for the integrity of Cajal bodies. *Mol Biol Cell.* 2006; 17:3221–31. [PubMed: 16687569]
28. Walker MP, Tian L, Matera AG. Reduced viability, fertility and fecundity in mice lacking the cajal body marker protein, coilin. *PLoS One.* 2009; 4:e6171. [PubMed: 19587784]
29. Strzelecka M, Trowitzsch S, Weber G, Luhrmann R, Oates AC, Neugebauer KM. Coilin-dependent snRNP assembly is essential for zebrafish embryogenesis. *Nat Struct Mol Biol.* 2010; 17:403–9. [PubMed: 20357773]
30. Collier S, Pendle A, Boudonck K, van Rij T, Dolan L, Shaw P. A Distant Coilin Homologue Is Required for the Formation of Cajal Bodies in *Arabidopsis*. *Mol Biol Cell.* 2006
31. Fischer U, Liu Q, Dreyfuss G. The SMN-SIP1 complex has an essential role in spliceosomal snRNP biogenesis. *Cell.* 1997; 90:1023–1029. [PubMed: 9323130]
32. Pellizzoni L, Kataoka N, Charroux B, Dreyfuss G. A novel function for SMN, the spinal muscular atrophy disease gene product, in pre-mRNA splicing. *Cell.* 1998; 95:615–24. [PubMed: 9845364]
33. Hebert MD, Szymczyk PW, Shpargel KB, Matera AG. Coilin forms the bridge between Cajal bodies and SMN, the spinal muscular atrophy protein. *Genes Dev.* 2001; 15:2720–9. [PubMed: 11641277]
34. Jady BE, Darzacq X, Tucker KE, Matera AG, Bertrand E, Kiss T. Modification of Sm small nuclear RNAs occurs in the nucleoplasmic Cajal body following import from the cytoplasm. *Embo J.* 2003; 22:1878–88. [PubMed: 12682020]
35. Nescic D, Tanackovic G, Kramer A. A role for Cajal bodies in the final steps of U2 snRNP biogenesis. *J Cell Sci.* 2004; 117:4423–33. [PubMed: 15316075]
36. Baillat D, Hakimi MA, Naar AM, Shilatifard A, Cooch N, Shiekhhattar R. Integrator, a multiprotein mediator of small nuclear RNA processing, associates with the C-terminal repeat of RNA polymerase II. *Cell.* 2005; 123:265–76. [PubMed: 16239144]
37. Egloff S, O'Reilly D, Chapman RD, Taylor A, Tanzhaus K, Pitts L, Eick D, Murphy S. Serine-7 of the RNA polymerase II CTD is specifically required for snRNA gene expression. *Science.* 2007; 318:1777–9. [PubMed: 18079403]

38. Frey MR, Matera AG. Coiled Bodies Contain U7 Small Nuclear RNA and Associate with Specific DNA Sequences in Interphase Cells. *Proc Natl Acad Sci USA*. 1995; 92:5915–5919. [PubMed: 7597053]
39. Smith K, Carter K, Johnson C, Lawrence J. U2 and U1 snRNA gene loci associate with coiled bodies. *J Cell Biochem*. 1995; 59:473–485. [PubMed: 8749717]
40. Frey MR, Bailey AD, Weiner AM, Matera AG. Association of snRNA genes with coiled bodies is mediated by nascent snRNA transcripts. *Curr Biol*. 1999; 9:126–131. [PubMed: 10021385]
41. Frey MR, Matera AG. RNA-mediated interaction of Cajal bodies and U2 snRNA genes. *J Cell Biol*. 2001; 154:499–509. [PubMed: 11489914]
42. Suzuki T, Izumi H, Ohno M. Cajal body surveillance of U snRNA export complex assembly. *J Cell Biol*. 2010; 190:603–12. [PubMed: 20733056]
43. Theimer CA, Jady BE, Chim N, Richard P, Breece KE, Kiss T, Feigon J. Structural and functional characterization of human telomerase RNA processing and cajal body localization signals. *Mol Cell*. 2007; 27:869–81. [PubMed: 17889661]
44. Cristofari G, Adolf E, Reichenbach P, Sikora K, Terns RM, Terns MP, Lingner J. Human telomerase RNA accumulation in Cajal bodies facilitates telomerase recruitment to telomeres and telomere elongation. *Mol Cell*. 2007; 27:882–9. [PubMed: 17889662]
45. Box JA, Bunch JT, Tang W, Baumann P. Spliceosomal cleavage generates the 3' end of telomerase RNA. *Nature*. 2008; 456:910–4. [PubMed: 19052544]
46. Bellini M, Gall JG. Coilin can form a complex with the U7 small nuclear ribonucleoprotein. *Mol Biol Cell*. 1998; 9:2987–3001. [PubMed: 9763457]
47. Broome HJ, Hebert MD. In Vitro RNase and Nucleic Acid Binding Activities Implicate Coilin in U snRNA Processing. *PLoS One*. 2012; 7:e36300. [PubMed: 22558428]
48. Velma V, Carrero ZI, Allen CB, Hebert MD. Coilin levels modulate cell cycle progression and γ H2AX levels in etoposide treated U2OS cells. *FEBS letters*. 2012
49. Weinberg RA, Penman S. Small molecular weight monodisperse nuclear RNA. *J Mol Biol*. 1968; 38:289–304. [PubMed: 5718554]
50. Spector DL, Lark G, Huang S. Differences in snRNP localization between transformed and nontransformed cells. *Mol Biol Cell*. 1992; 3:555–569. [PubMed: 1535243]
51. Toyota CG, Davis MD, Cosman AM, Hebert MD. Coilin phosphorylation mediates interaction with SMN and Smb⁺. *Chromosoma*. 2009
52. Sun J, Xu H, Subramony SH, Hebert MD. Interactions between Coilin and PIASy partially link Cajal bodies to PML bodies. *J Cell Sci*. 2005; 118:4995–5003. [PubMed: 16219678]
53. Hebert MD, Matera AG. Self-association of coilin reveals a common theme in nuclear body localization. *Mol Biol Cell*. 2000; 11:4159–71. [PubMed: 11102515]
54. Toyota CG, Davis MD, Cosman AM, Hebert MD. Coilin phosphorylation mediates interaction with SMN and Smb⁺. *Chromosoma*. 2010; 119:205–15. [PubMed: 19997741]
55. Carrero ZI, Velma V, Douglas HE, Hebert MD. Coilin phosphomutants disrupt cajal body formation, reduce cell proliferation and produce a distinct coilin degradation product. *PLoS One*. 2011; 6:e25743. [PubMed: 21991343]
56. Otzen DE, Oliveberg M. A simple way to measure protein refolding rates in water. *J Mol Biol*. 2001; 313:479–83. [PubMed: 11676533]
57. Hearst SM, Gilder AS, Negi SS, Davis MD, George EM, Whittom AA, Toyota CG, Husedzinovic A, Gruss OJ, Hebert MD. Cajal-body formation correlates with differential coilin phosphorylation in primary and transformed cell lines. *J Cell Sci*. 2009; 122:1872–81. [PubMed: 19435804]

HIGHLIGHTS

- What is the relationship between coilin and RNAs, specifically telomerase RNA processing?
- We report a specific in vivo association between coilin and rRNA, U snRNA and telomerase RNA.
- We also show a change in RNA association upon cellular stress by cisplatin and etoposide.
- Additionally, we provide evidence of coilin involvement in telomerase RNA biogenesis.
- We provide evidence of a more operative role of coilin in RNA biogenesis, aside from its function in Cajal body integrity.

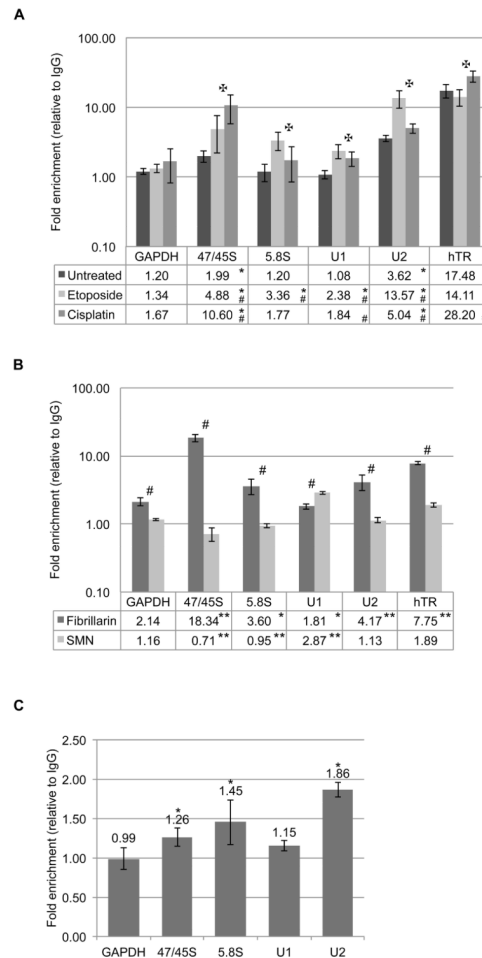


Figure 1.

(A) Histogram of RNA IP results with IgG and α -coilin from untreated, etoposide or cisplatin treated HeLa cells; fold enrichment of α -coilin IP over IgG control is shown on \log_{10} scale; error bars represent 1 s.d. for 3 experimental repeats with 3 technical repeats each; * indicates $p < 0.005$ relative to GAPDH within a treatment; # indicates $p < 0.002$ relative to untreated cells within a primer set; * indicates $p < 0.04$ between etoposide and cisplatin within a primer set. (B) Histogram of RNA IP results with IgG, α -fibrillarin and α -SMN from HeLa cells; fold enrichment over IgG control is shown on \log_{10} scale; error bars represent 1 s.d. for 1–3 experimental repeats per primer and 3 technical repeats per experiment; * indicates $p < 0.05$ and ** $p < 0.001$ relative to GAPDH within an IP; # indicates $p < 0.02$ between IPs for the same primer set. (C) Histogram of RNA IP results with IgG and α -coilin from WI-38 cells; fold enrichment of α -coilin over IgG is shown; error bars represent 1 s.d. for 2 experimental repeats with 3 technical repeats each; * indicates $p < 0.01$ relative to GAPDH.

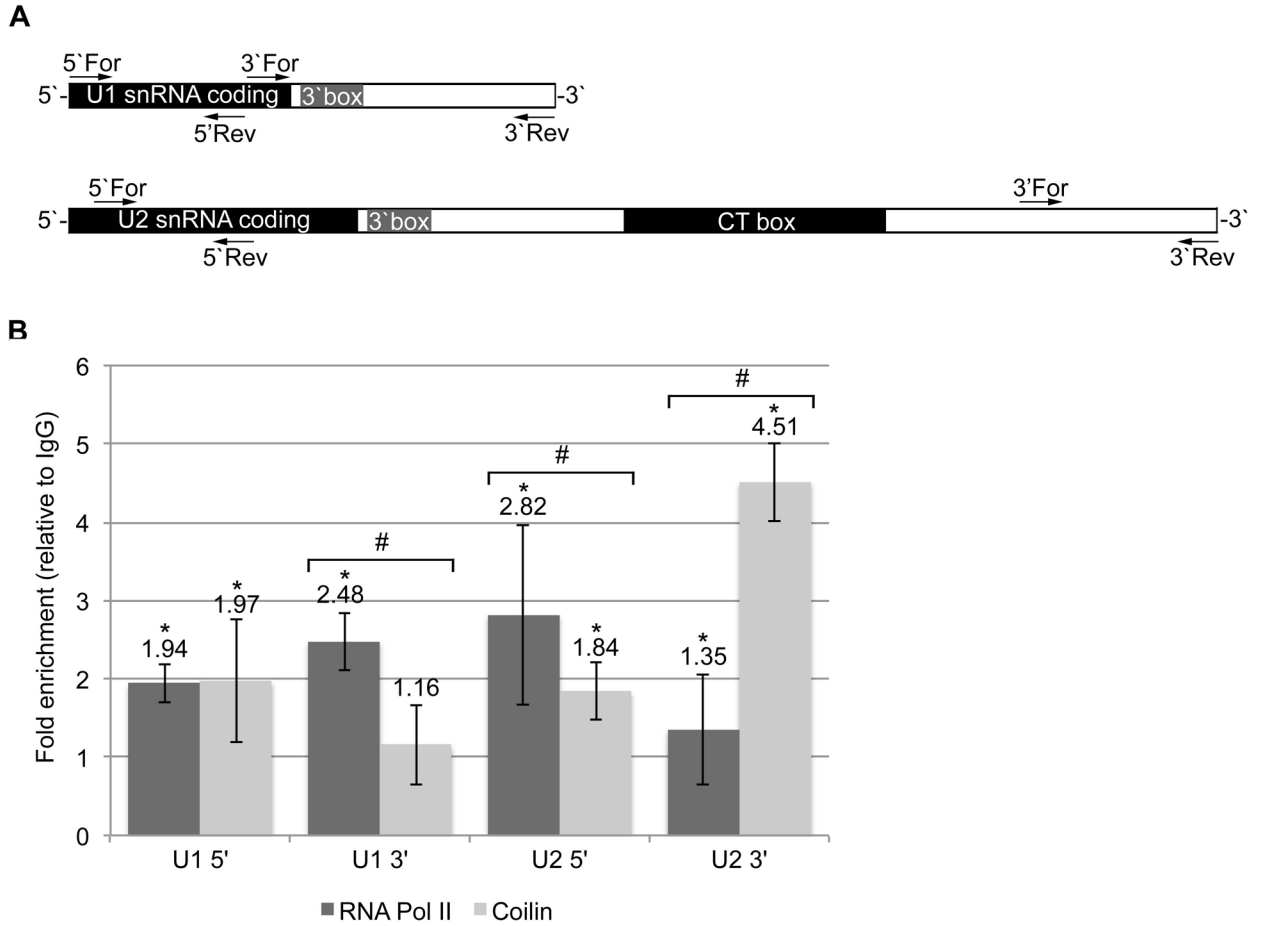


Figure 2. (A) Diagram showing primer binding locations within the target regions of the U1 and U2 snRNA gene loci. (B) Histogram of ChIP results using antibodies to coilin and RNA polymerase II in HeLa cells, fold enrichment of α -coilin and α -RNA polymerase II over IgG control is shown; * indicates $p < 0.005$ relative to IgG; # above data set for a primer pair indicates $p < 0.01$ between coilin and RNA polymerase II IPs. Error bars represent 1 s.d. for 3 experimental repeats with 3 technical repeats each.

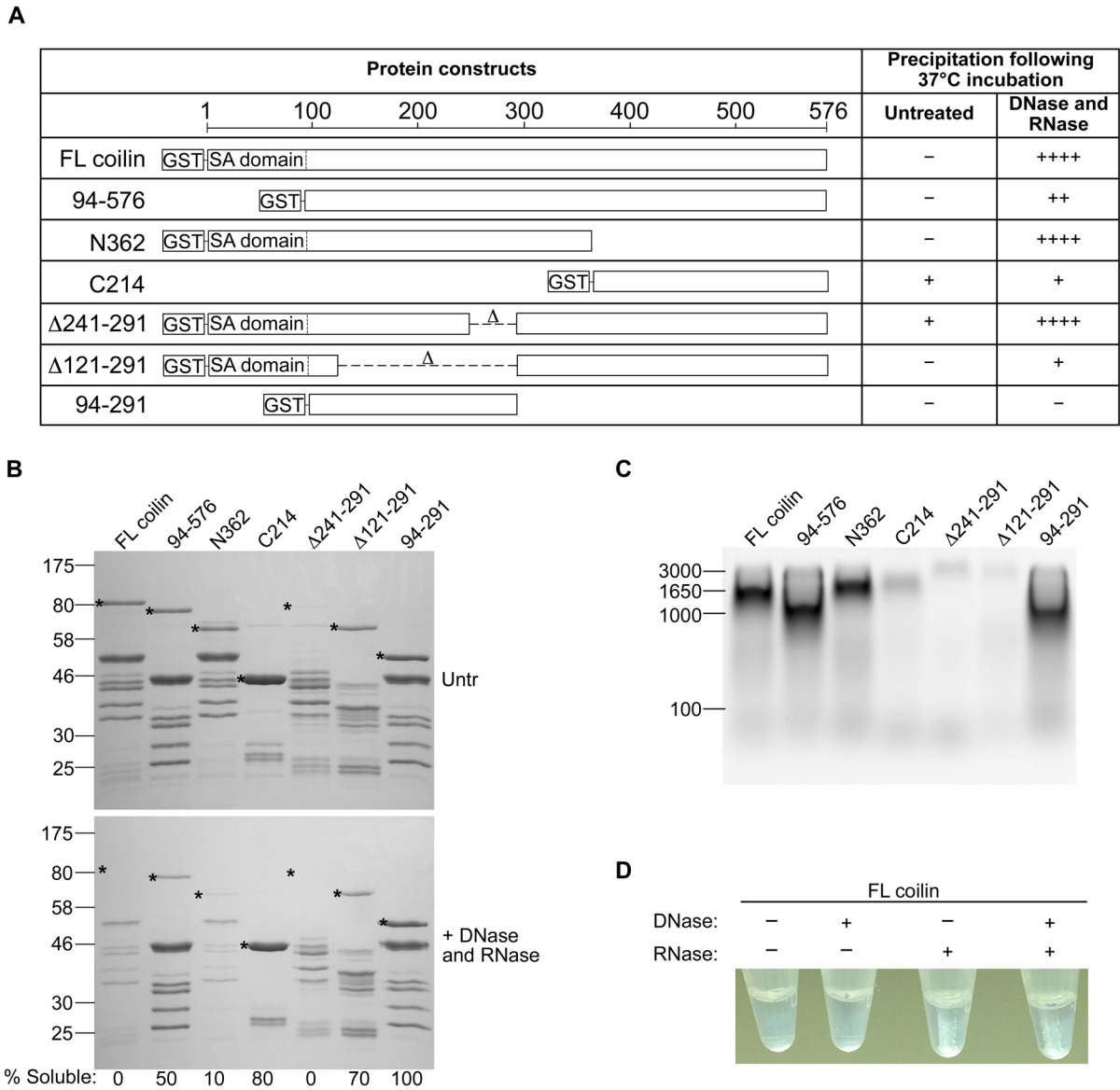


Figure 3.

(A) Diagrams of seven GST-tagged coilin constructs showing precipitation behavior of equal total protein, 160 μ g, following incubation with or without DNase and RNase, with “-” being no visible precipitation and “++++” the most relative precipitate; SA = self-association, FL = full length. (B) *Top panel*, Coomassie stained SDS-PAGE gel of equal total partially purified GST-tagged proteins untreated; *Bottom panel*, equal volume of soluble protein following incubation with DNase and RNase; * indicates full length GST-tagged protein of interest for each construct; % Soluble value indicates the percentage of soluble protein remaining after nuclease treatment, relative to untreated soluble protein, as calculated by relative densitometric analysis of protein bands in top and bottom panels. (C) Equal amounts of total GST-tagged protein loaded into an agarose gel and stained with ethidium bromide to visualize relative amounts of co-purified nucleic acid. (D) Representative image of visible precipitate which forms upon nuclease treatment, seen with RNase treatment or the combination of DNase and RNase.

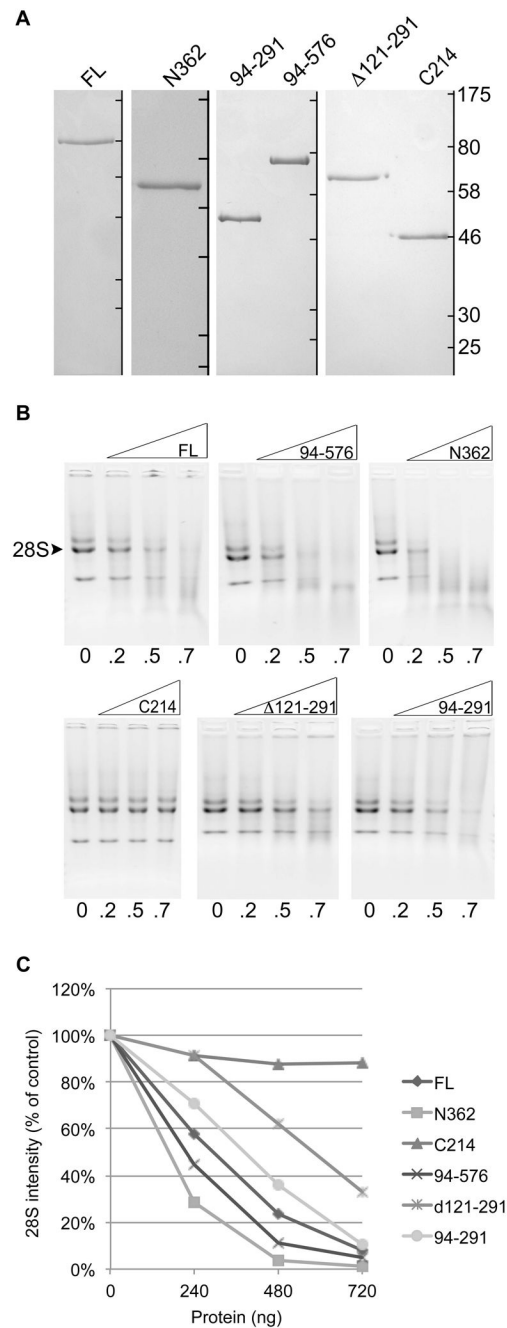
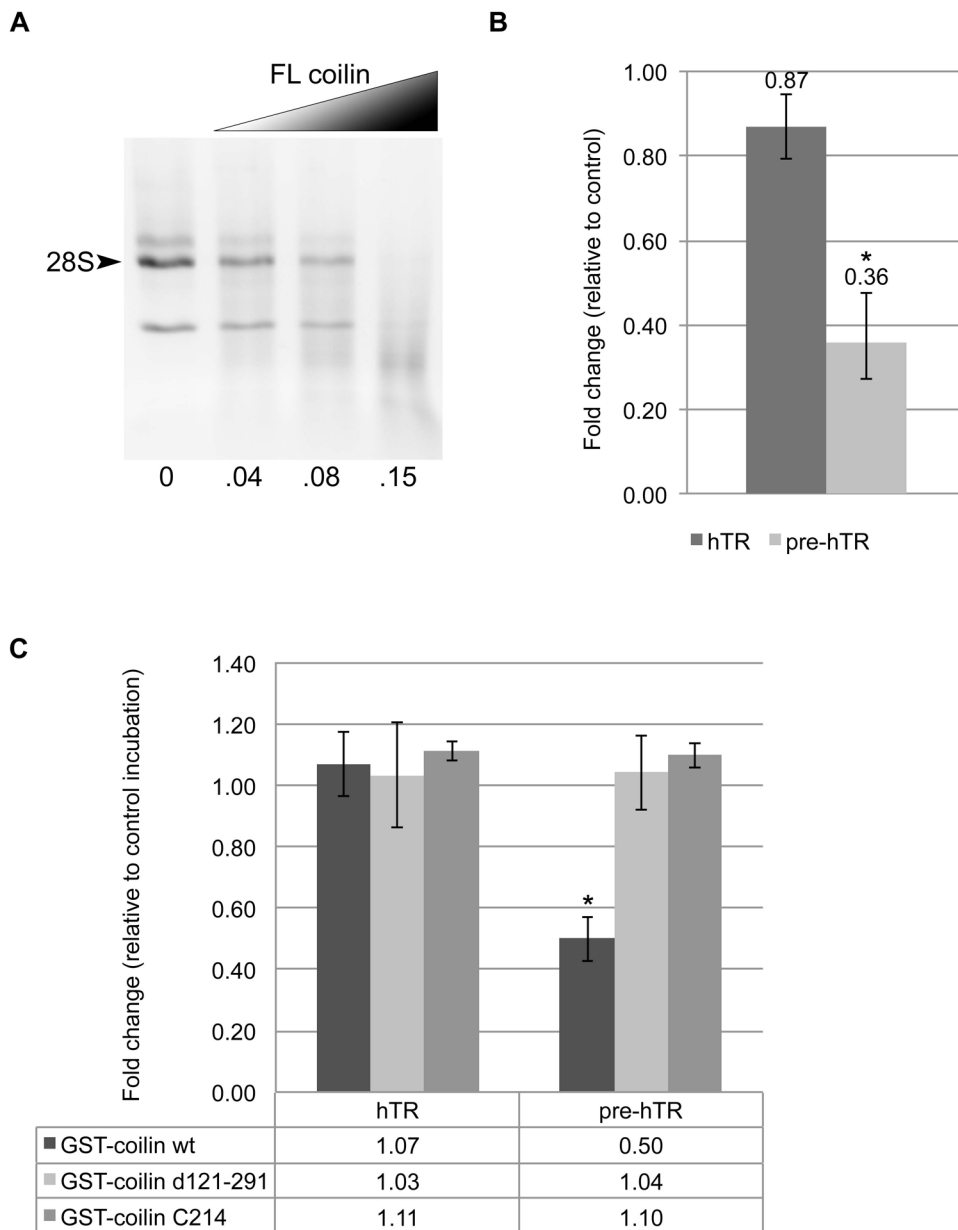


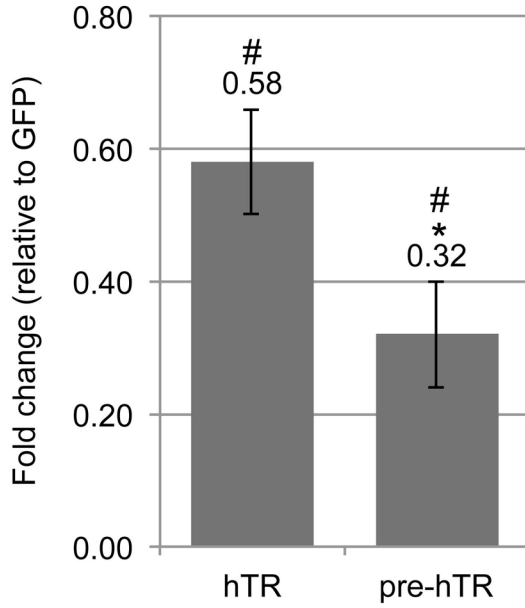
Figure 4.

(A) Coomassie stained SDS-PAGE gels containing fully purified nucleic acid-free GST-tagged proteins; ladder to the right of each separate panel denotes marker locations of 175, 80, 58, 46, 30 and 25 kDa for each individual gel. (B) Agarose gels containing RNase assay results visualized by ethidium bromide; 500 ng RNA per lane; numbers beneath lanes indicate amount of protein in μ g; the 28S rRNA band is indicated, with both the 32S and 18S also visible. (C) Line graph showing densitometric analysis of the 28S rRNA bands from images shown in B; percent band density of the control (no protein) band is plotted for each protein and amount.

**Figure 5.**

(A) RNase activity of nucleic acid free purified coilin with 500 ng RNA; numbers beneath lanes indicate amount of protein in μg . (B) Histogram showing the fold change relative to control reactions of hTR and pre-hTR levels following incubation of HeLa RNA with nucleic acid free purified coilin; * indicates $p < 0.05$ relative to the control incubation. (C) Histogram showing the fold change relative to control reactions of hTR and pre-hTR levels following incubation of HeLa RNA with nucleic acid free purified GST-tagged coilin proteins; * indicates $p < 2.0\text{E-}9$ relative to GST-coilin d121-291 and GST-coilin C214. Error bars represent 1 s.d. for 3 experimental repeats with 3 technical repeats each.

A



B

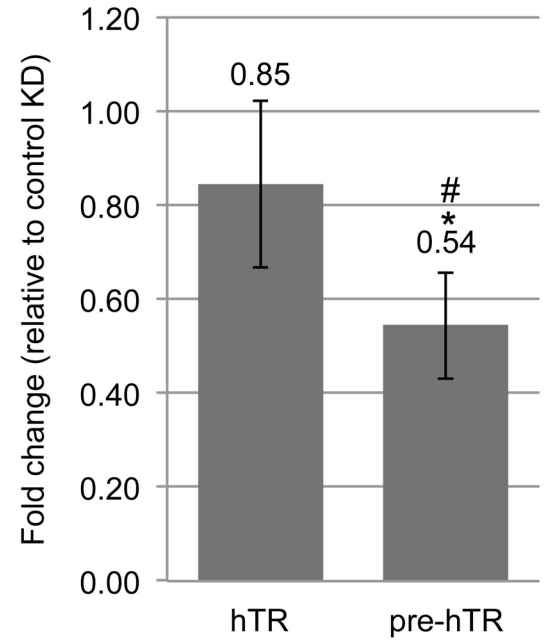


Figure 6.

(A) Histogram showing the fold change relative to GFP transfection of hTR and pre-hTR levels following a 24h transfection with GFP-coilin wt; # indicates $p < 2E-6$ and * indicates $p < 2E-8$ relative to total hTR. (B) Histogram showing the fold change relative to control knockdown of hTR and pre-hTR levels following a 48h coilin knockdown in HeLa cells resulting in 89% reduction of coilin mRNA; # indicates $p < 6E-5$ relative to control KD and * indicates $p < 0.001$ relative to total hTR. Error bars represent 1 s.d. for 3 experimental repeats with 3 technical repeats each.